Published in final edited form as:
Clin Exp Metastasis. 2010 April ; 27(4): 241–249. doi:10.1007/s10585-010-9322-3.

GPR56 Plays Varying Roles in Endogenous Cancer Progression

Lei Xu[1,4,#], **Shahinoor Begum**[1], **Marc Barry**[1,5], **Denise Crowley**[1], **Liquan Yang**[3], **Roderick T. Bronson**[2], and **Richard O. Hynes**[1]

[1]Howard Hughes Medical Institute, the Koch Institute for Integrative Cancer Research, Massachusetts Institute of Technology, Cambridge, MA 02193

[2]Department of Biomedical Sciences, Tufts University School of Veterinary Medicine, North Grafton, Massachusetts

[3]Department of Biomedical Genetics, University of Rochester Medical Center, Rochester, NY 14642

Abstract

GPR56, a non-classical adhesion receptor, was previously reported to suppress tumor growth and metastasis in xenograft models using human melanoma cell lines. To understand whether GPR56 plays similar roles in the development of endogenous tumors, we analyzed cancer progression in *Gpr56−/−* mice using a variety of transgenic cancer models. Our results showed that GPR56 suppressed prostate cancer progression in the TRAMP model on a mixed genetic background, similar to its roles in progression of melanoma xenografts. However, its roles in other cancer types appeared to be complex. It had marginal effects on tumor onset of mammary tumors in the MMTV-PyMT model, but had no effects on subsequent tumor progression in either the MMTV-PyMT mice or the melanoma model, *Ink4a/Arf−/− tyr-Hras*. These results indicate diverse roles of GPR56 in cancer progression and provide the first genetic evidence for the involvement of an adhesion GPCR in endogenous cancer development.

Keywords

GPR56; prostate cancer; breast cancer; melanoma; animal models on cancer

Introduction

Tumor growth and metastasis involve multiple interactions between cells and extracellular matrix (ECM). These interactions are mediated by adhesion receptors, which bind to ECM components and transmit bi-directional signals across the cytoplasmic membrane to influence proliferation, migration and invasion of cancer cells [1]. The prototypic adhesion receptors are integrins [2], heterodimeric receptors that are formed by selective pairing between the 18 α and 8 β subunits. The different integrins exhibit variable affinities for a large number of ECM proteins, and not only transmit signals vertically across the cytoplasmic membrane, but also laterally to other adhesion receptors, such as tetraspanin proteins, dystroglycans, and syndecans [3]. These multi-dimensional interactions among adhesion receptors are thought to profoundly influence cell behaviors during cancer progression, but how that occurs remains unclear and needs further investigation [4].

[#]Correspondence: lei_xu@urmc.rochester.edu; telephone: 585-273-1302; fax: 585-273-1450.
[4]Current address: Department of Biomedical Genetics, University of Rochester Medical Center, Rochester, NY 14642;
[5]Current address: Dept. of Pathology, MSC084640, 1 University of New Mexico, Albuquerque, NM 87131-0001

GPR56 is a member of a newly defined family of adhesion receptors. Called adhesion G protein-coupled receptors (GPCRs) [5], they are believed to mediate both G protein-coupled signaling and cell adhesion – functions attributed to their seven-pass transmembrane domain, similar to those in conventional GPCRs, and the adhesion motifs present in their long N-termini. Over 30 members of adhesion GPCRs exist in mammals [5] and some have been shown to interact with ECM [6–8] and regulate cell adhesion [9,10], but the majority of their functions have remained unexplored. The roles of GPR56 in cell-ECM interactions have been established through biochemical and genetic studies. The N-terminus of GPR56 was found to bind directly to tissue transglutaminase (TG2), a major crosslinking enzyme in ECM [8]. TG2 modulates the biochemical and biophysical properties of ECM through its crosslinking activity as well as its crosslinking-independent activities [11,12]. Therefore GPR56 might regulate ECM properties and cell-ECM interactions through its association with TG2. In addition, disruptions of ECM assembly in both cerebrum and cerebellum were observed in *Gpr56*−/− mice [13,14], and *Gpr56*−/− cerebellar granular cells exhibit reduced adhesion to laminin, a constitutive ECM component in the basement membrane [14], further suggesting a critical role of GPR56 in cell-ECM adhesion.

Consistent with its effects on cell adhesion, GPR56 has been implicated in cancer progression. Its expression levels were inversely correlated with the metastatic potentials of human melanoma cell lines [8,15], and its re-expression led to suppressed melanoma growth and metastasis in a xenograft cancer model [8], indicating an inhibitory role for GPR56 in cancer progression. However, the expression levels of GPR56 were reportedly increased in cancerous lesions compared with those in adjacent normal tissues in several cancer types [16,17], suggesting that GPR56 might play a promoting role at the early stages of cancer development.

To further understand the roles of GPR56 in cancer development, we analyzed endogenous cancer progression in *Gpr56*−/− mice using transgenic cancer models. Transgenic cancer models, in which an oncogene is expressed under the control of a tissue-specific promoter [18], have increasingly been shown to more accurately recapitulate cancer progression than do xenograft tumor models. By analyzing the contribution of GPR56 in the transgenic models for three major cancer types, prostate cancer (TRAMP) [19], breast cancer (MMTV-PyMT) [20], and melanoma (*Ink4a/Arf*−/− *Tyr-HRAS*) [21], we found that GPR56, an adhesion GPCR, plays diverse roles in endogenous cancer progression.

Materials and Methods

Animals

Gpr56 knock-out mice were obtained from Genentech, Inc. They were originally generated in 129/BL/6 background, viable and fertile. They were subsequently crossed with a Balb/c mouse before being bred with MMTV-PyMT/FvB mice for studies on mammary tumors. Therefore, the offspring are in a mixed genetic background comprising 129/BL/6/FvB/Balb/c. Because the transgenic females died during pregnancy, we crossed the transgenic F1 males (*Gpr56*+/− MMTV-PyMT) with their non-transgenic *Gpr56*+/− female siblings or cousins to obtain *Gpr56*+/+ MMTV-PyMT, *Gpr56*+/− MMTV-PyMT, and *Gpr56*−/− MMTV-PyMT mice for tumor studies. A palpation test was performed once a week to measure tumor onset when mice were between 4–14 weeks old. The mice were subsequently sacrificed, and their mammary glands were weighed and fixed in formalin for histological study or frozen in O.C.T (Sakura Finetek USA, Inc., CA) for immunohistochemical analyses. Their lungs were also harvested and macroscopic metastases were counted under a dissecting microscope.

For the prostate cancer study, we crossed the *Gpr56+/−* mice in the mixed genetic background, as mentioned above, with TRAMP mice, which are in pure C57Bl/6 background. Since the male offspring develop prostate cancer, we crossed the F1 transgenic females (*Gpr56+/−* TRAMP) with non-transgenic male siblings or cousins *(Gpr56+/−)* to obtain transgenic mice in a *Gpr56+/+*, *Gpr56+/−*, or *Gpr56−/−* background. The mice were sacrificed at 20 weeks, and their prostates were fixed in formalin for histological analyses or frozen in O.C.T for immunohistochemical analyses. The para-lumbar lymph nodes were dissected and weighed. The ones that are not detectable by the scale were considered as 0.001g.

To test whether the effects of GPR56 on prostate cancer progression was strain-specific, we backcrossed the *Gpr56* knock-out mice into the C57BL/6 background for five generations and then crossed them again with TRAMP mice. The mice were sacrificed at 25 weeks and their prostates were weighed and fixed in formalin for histological analyses. Their para-lumbar lymph nodes were also harvested and weighed.

To examine the role of GPR56 in melanoma progression, *Gpr56−/−* mice was crossed into the FvB background for five generations and subsequently crossed with male *Ink4a/Arf−/− tyr-Hras* mice. The *tyr-Hras* transgene was inserted in Y-chromosome in the *Ink4a/Arf−/− tyr-Hras* mice and therefore all the transgenic mice are male. The male *Gpr56+/− Ink4a/Arf +/−* offspring from the above crosses were bred with their female *Gpr56+/− Ink4a/Arf+/−* siblings or cousins, and the male *Gpr56−/− Ink4a/Arf−/−* progeny in the next generation were bred with either *Gpr56−/− Ink4a/Arf−/−* females or *Gpr56+/− Ink4a/Arf−/−* females to obtain *Gpr56−/− Ink4a/Arf−/− tyr-Hras* or *Gpr56+/− Ink4a/Arf−/− tyr-Hras* mice. The appearance of macroscopic melanoma-like lesions in these mice was monitored weekly by visual inspection beginning at 4 weeks of age. The date of first detection of melanomas was recorded as the onset of melanoma. The mice were monitored weekly for their health status by one of us (S.B.) and were sacrificed when moribund. Their ages at the termination date were recorded as their lengths of survival. All the melanomas were subsequently harvested and weighed.

All procedures were performed in accordance with the Massachusetts Institute of Technology Division of Comparative Medicine animal care guidelines.

Histology and Immunohistochemistry

Tissues from the TRAMP, MMTV-PyMT, and *Ink4a/Arf −/−* tyr-Hras mice were collected and processed as described above. For histological analyses, 4 μm sections were cut and stained with hematoxylin and eosine. The staining patterns were viewed and evaluated by board-certified pathologists (M.B. and R.B.) for the extent of tumor progression. Prostate tumors from TRAMP mice were graded blindly by one of the pathologists (M.B.), based on reported grading criteria [22].

For immunohistochemical analyses, prostates were fresh frozen in O.C.T. and cut into 6 μm sections. Each section was incubated with an antibody against the C-terminus of GPR56 (anti-GPRC antibody, 1:500) [8] at 4 degrees overnight, followed by the Alex 488-conjugated donkey anti-rabbit secondary antibody. Images were captured by the SPOT camera and processed with the AdobePhotoshop Software.

Western Blots

Tumor lysates from prostate cancer cell lines were prepared as reported previously [23]. Other tissues were homogenized in RIPA buffer on ice. After centrifugation at 13, 000 rpm for 30 min, the supernatant of each lysate was separated on a 4–20% SDS-polyacrylamide gel and probed with the anti-GPRC antibody (1:200), followed by detection with HRP-

conjugated donkey anti-rabbit secondary antibody. The same immunoblot was probed with mouse anti-GAPDH antibody to measure the total amount of protein in each lysate. To compare the expression levels of GPR56 in the tumor samples from the prostate cancer cell lines, the intensities of the GPR56 and GAPDH bands from each sample were measured using the AlphaImager Gel Imaging System (Alpha Innotech, CA). After being normalized to the intensity of the GAPDH signal, the ratio of the intensity of GPR56 in each sample over that in the parental line (P) was calculated and used as the relative intensity score.

Graphs and Statistical Analyses

S-plus software was used to generate the curves for survival probability and tumor onset from the *Ink4a/Arf−/− tyr-Hras* mice and perform the log-rank tests to assess the statistical difference between the curves. Microsoft Excel was used to generate the remaining graphs in the manuscript. In order to determine which statistical methods should be used to assess the statistical difference among the data, the normality of data distribution was evaluated by KS normality test, D'Agostino & Pearson omnibus normality test, and Shapiro-Wilk normality test (Graphpad, CA). The data on tumor onset from the MMTV-PyMT *Gpr56*+/+ and MMTV-PyMT *Gpr56*+/− mice, and the tumor weights from the MMTV-PyMT *Gpr56*+/+ were the only data that passed all the three tests and were considered normally distributed (data not shown). The statistical difference of tumor onsets between the MMTV-PyMT *Gpr56*+/+ and MMTV-PyMT *Gpr56*+/− mice was consequently analyzed by the *Student t*-test (http://www.physics.csbsju.edu/stats/t-test.html). All the rest of comparisons were analyzed by the non-parametric *Mann-Whitney* test (http://elegans.swmed.edu/~leon/stats/utest.html), since at least one set of data in each comparison did not meet the criteria of Gaussian distribution.

Results

GPR56 expression in prostate cancer from xenograft and TRAMP mouse models

We reported previously a down-regulation of GPR56 expression in highly metastatic human melanoma cell lines. Re-expression of GPR56 led to suppressed melanoma growth and metastasis. To examine whether this also holds true in prostate cancer, we analyzed the expression levels of GPR56 in tumor samples from prostate cancer cell lines with different metastatic potentials. Prostate cancer cell lines, #78, pMicro, and #82 were derived from the parental PC-3 cell line and selected based on their ability to spread to lung, as reported [23]. Cell line #78 and the parental line were both poorly metastatic, the pMicro line had intermediate metastatic potential, and the #82 line had the highest metastatic potential. Subcutaneous tumors derived from these cell lines were transplanted into mouse prostates. The orthologous transplants were subsequently harvested and lysed for western blot analyses using an antibody against GPR56. Significant reduction of GPR56 expression was observed in tumor lysates from the metastatic pMicro and #82 cell lines compared with those from the poorly metastatic #78 and parental lines (Figure 1A), suggesting that in prostate cancer, as in melanoma, GPR56 expression is inversely correlated with the metastatic potential of cancer cells.

Whether GPR56 expression changes during spontaneous prostate cancer progression was examined using TRAMP (TRansgenic Adenocarcinoma of the Mouse Prostate) mice. TRAMP mice express the SV40 T antigen under the rat probasin promoter, which is active specifically in prostate epithelium. Prostate cancer in TRAMP mice progresses from prostate intraepithelial neoplasia (PIN) to undifferentiated carcinoma, and eventually metastasizes to lymph nodes, similar to prostate cancer in humans [24]. Prostate tumors from TRAMP mice were graded based on their histology, with normal prostate as grade 1 and undifferentiated adenocarcinoma as grade 5 [22]. We determined the expression levels of GPR56 in prostates

from TRAMP mice by both western blot analyses and immunofluorescence staining. The results showed that GPR56 was expressed at a low level in normal prostate and well-differentiated adenocarcinoma, but at a significantly higher level in poorly differentiated adenocarcinoma (Figure 1B and C) and in metastases (Figure 1D). This is in contrast to its down-regulation in metastatic prostate cancer cell lines (Figure 1A), suggesting that GPR56 might play different roles at different stages of prostate cancer progression, or its functions in prostate xenografts and endogenous prostate cancer differ (see Discussion).

Prostate cancer progression in TRAMP mice on a mixed genetic background was enhanced in *Gpr56−/−* mice relative to that in *Gpr56+/+* mice

To directly examine the roles of GPR56 in endogenous prostate cancer progression, we crossed *Gpr56−/−* mice (which were in a mixed genetic background, see Materials and Methods) with TRAMP mice. The male *Gpr56+/+*, *Gpr56+/−*, and *Gpr56−/−* offspring were analyzed for prostate cancer progression at the age of 20 weeks. All mice carrying the SV40 transgene developed prostate cancer by this age (Supplementary Figure 1), but prostate tumors from the *Gpr56−/−* mice showed significantly increased tumor burden (Figure 2A, $p < 0.01$, *Mann-Whitney* test), more advanced histological grades (Figure 2B, $p = 0.05$, *Fisher Exact* test), and gave rise to increased weights of lymph node metastases (Figure 2C, $p < 0.01$, *Mann-Whitney* test) than those from wild-type mice, suggesting strongly that GPR56 suppresses the progression of prostate cancer in TRAMP mice on a mixed genetic background.

Prostate cancer progression in TRAMP mice has been shown to be strain-specific, with mice on the FvB/N background being more susceptible than those on the C57BL/6 background [25]. The mice analyzed as described above were on a mixed genetic background, thus it is possible that FvB/N background was over-represented in *Gpr56+/−* and *Gpr56−/−* offspring relative to those in the *Gpr56+/+* offspring, leading to a skewed impression of enhanced prostate cancer progression in *Gpr56+/−* and *Gpr56−/−* mice. To address this issue, the *Gpr56−/−* mice were backcrossed with C57BL/6 mice for five generations before being crossed again with TRAMP mice. The male offspring that carried the SV40 transgene were analyzed at the age of 25 weeks. Although all animals had developed prostate cancer, no significant difference in tumor weights (Figure 3A), tumor grades (Figure 3B), or lymph node metastases (data not shown) was observed among the *Gpr56+/+*, *Gpr56+/−*, and *Gpr56−/−* mice. These results are consistent with the possibility that the enhanced cancer progression in *Gpr56−/−* mice of mixed background is due to an over-represented FvB/N background in these mice relative to that in the *Gpr56+/+* mice. An alternative explanation is that the GPR56-mediated inhibition of prostate cancer progression is specific to a particular genetic background (see more in Discussion).

GPR56 had marginal effects on mammary tumor progression in MMTV-PyMT mice

To investigate whether GPR56 plays any roles in mammary tumor progression, *Gpr56−/−* mice of mixed genetic background were crossed with MMTV-pyMT mice (which were in the FvB background). The offspring were analyzed for tumor onset, progression, and metastasis. MMTV-PyMT mice express the polyoma middle T oncogene under the control of mouse mammary tumor virus promoter, which induces mammary tumors that metastasize to lung [20]. As in the prostates of TRAMP mice, the expression level of GPR56 was not detectable in normal mammary glands, but was significantly increased in mammary carcinoma induced by the polyoma middle T oncogene (Figure 4A).

The increase in GPR56 expression in mammary tumor cells relative to normal tissue suggested that it might play a role in cancer cell transformation. To test this, the onset of tumorigenesis in MMTV-PyMT mice was determined by weekly palpation starting at the

age of 4 weeks. The results indicated a significant delay in tumor onset in *Gpr56+/−* mice relative to that of wild-type mice (Figure 5B). However, tumor onset in *Gpr56−/−* mice fell in between the tumor onsets of *Gpr56+/−* and *Gpr56+/+* mice and did not differ significantly from either, suggesting that GPR56 might have marginal effects on initiation of mammary cancer in this model. The effects of GPR56 on later stages of mammary tumor progression and metastasis were analyzed by measuring mammary gland weights, tumor grades, and the number of lung metastases in the MMTV-PyMT mice at the age of 14 weeks. No significant difference was found among the *Gpr56+/+*, *Gpr56+/−*, and *Gpr56−/−* mice (Figure 4C and D, Supplementary Figure 2), suggesting that GPR56 does not affect later stages of mammary cancer progression in MMTV-PyMT mice.

GPR56 did not affect melanoma progression in *Ink4a/Arf−/− tyr-Hras* mice

Our previous study showed that GPR56 suppresses melanoma metastasis and growth in a xenograft metastasis model. To investigate whether GPR56 also affects endogenous melanoma progression, we crossed *Gpr56−/−* mice (backcrossed into FvB/N background for five generations) with the melanoma model *Ink4a/Arf−/− tyr-Hras; FvB/N* mice, which are null for the *Ink4a*/*Arf* locus and express the oncogene HRAS under the control of the melanocyte-specific tyrosinase promoter. Loss of *Ink4a* has been linked to melanoma development in humans [26], and, in combination with the loss of *Arf* and the expression of HRAS in melanocytes, induces the development of melanoma in mice [21].

GPR56 protein was expressed in melanoma samples from *Ink4a/Arf−/− tyr-Hras* mice (Figure 5A), but the *Gpr56+/+*, *Gpr56+/−*, and *Gpr56−/−* mice carrying the transgenes did not differ in the tissue distribution and histology of melanomas (Supplementary Figure 3), tumor onset (Figure 5B), length of survival (Figure 5C), or the lag between tumor onset and death (data not shown). The tumor burden at the time of death also did not differ among these mice (Figure 5D), suggesting that GPR56 does not affect melanoma progression in *Ink4a/Arf−/− tyr-Hras* mice.

Discussion

GPR56 is a member of the adhesion GPCR family. Consistent with their predicted roles as adhesion receptors, several adhesion GPCRs have been implicated in cancer development [8–10,27,28]. However, all of these studies used xenograft cancer models, and whether those adhesion GPCRs play similar roles in endogenous cancer progression has not been investigated. We report here our analyses on the involvement of GPR56 in endogenous cancer progression using *Gpr56−/−* mice and transgenic cancer models. We found that GPR56 plays diverse roles in endogenous cancer progression. GPR56 suppressed prostate cancer development in a background-dependent manner; it may have some effects on the onset of mammary tumors in MMTV-PyMT mice, but did not appear to affect the melanoma progression in *Ink4a/Arf −/− tyr-Hras* mice.

GPR56 was predicted to inhibit endogenous cancer progression, based our previous findings using xenograft models of melanoma [8]. Consistent with this prediction, the expression levels of GPR56 were inversely correlated with the metastatic potential of prostate cancer cell lines. In addition, endogenous prostate cancer progression in the TRAMP model with a mixed genetic background was significantly enhanced in *Gpr56−/−* mice compared with that in wild-type mice, suggesting that GPR56 suppresses prostate cancer progression in TRAMP mice.

The effects of GPR56 on prostate cancer progression in TRAMP mice appeared to be background-dependent, since effects on cancer development were only observed on a mixed genetic background but not on the pure C57BL/6 background. Several possibilities might

account for this difference. First, the FvB/N background may be over-represented in the *Gpr56*+/− and *Gpr56*−/− mice (relative to the *Gpr56*+/+ mice), resulting in an enhanced prostate cancer progression that is independent of GPR56. Alternatively, GPR56 might cooperate with a strain-specific modifier in the mixed genetic background that is not present in the C57BL/6 background to inhibit prostate cancer progression. Finally, the lack of effects on prostate cancer progression in C57BL/6 mice could also be due to developmental defects in *Gpr56*−/−; C57BL/6 mice. Our preliminary analyses suggest that *Gpr56*−/−; C57BL/6 mice are defective in testis development (unpublished data). Testis is the major organ that secretes testosterones, which are essential for prostate development and prostate cancer progression. Its dysfunction might therefore impede the otherwise enhanced prostate cancer progression in *Gpr56*−/− mice.

The mammary tumor onset in *Gpr56*+/− mice was significantly delayed relative to *Gpr56*+/+ mice, suggesting that GPR56 might promote mammary tumor onset in this model. However, no significant difference in tumor onsets was observed between *Gpr56*−/− mice and either *Gpr56*+/− or *Gpr56*+/+ mice, and considerable data scattering was present for all three groups, indicating that the effects of GPR56 on mammary tumor onset may be marginal and thus could be readily masked by the complexity of mixed genetic background.

In both TRAMP and MMTV-PyMT models, GPR56 expression was induced in the cancerous lesions relative to the adjacent normal tissues. Increased expression of GPR56 in primary tumors relative to normal tissues in human cancer has been reported [16,17] and was frequently shown in analyses from microarray data (www.oncomine.org). The most straightforward explanation is that GPR56 expression is induced during oncogenesis, although *Gpr56* has not been shown to be a direct target of any oncogene. An alternative explanation is that GPR56 is expressed in a minor population of cells in normal prostates and breasts, which are amplified during cancer progression. This minor population might represent cancer-initiating cells, i.e., cancer stem cells. GPR56 has been speculated to play roles in stem cells of normal tissues, since its expression was believed to be up-regulated in both neuronal and hematopoietic stem cells [29,30]. It is tempting to connect the potential roles of GPR56 in normal stem cells with its roles in cancer stem cells; however, more careful studies will be needed to address this issue.

The increased expression of GPR56 in poorly differentiated prostate tumors was in contrast to its down-regulation in highly metastatic prostate cancer cell lines. How this occurs needs to be investigated further. It is possible that GPR56 plays distinct roles at different stages of prostate cancer progression: it might promote prostate cancer progression in the primary tumors, but inhibit the establishment of metastases. Or, GPR56 may function differently in prostate xenografts than in endogenous prostate tumors.

In contrast to our conclusions from the xenograft models, GPR56 did not affect melanoma progression in *Ink4a/Arf*−/− *tyr-Hras* mice. This might be partly due to the characteristics of the *Ink4a/Arf*−/− *tyr-Hras* model. We observed significant variation in tumor onsets and progression among the *Ink4a/Arf*−/− *try-Hras* mice. This intrinsic variation might mask the effects of GPR56 on melanoma progression in these mice. In addition, the *Ink4a/Arf*−/− *try-Hras* mice die from lymphoma at various ages, making it difficult to assess the roles of GPR56 on melanoma at any fixed time point or at later developmental stages (during metastasis, for example).

Taken together, it is apparent from our study that GPR56 plays varying roles on spontaneous cancer progression. Although it is too early to predict the mechanism of its regulation on cancer, multiple lines of evidence suggest that GPR56 functions as an adhesion receptor and interacts with ECM directly. Its N-terminus binds to TG2, a major crosslinking enzyme in

the extracellular matrix [8,12], and *Gpr56*−/− mice possess defects in basement membrane assembly in both cerebrum and cerebellum [13,14]. However, we have not observed any overt differences in ECM deposition between *Gpr56*−/− tumors and *Gpr56*+/− or wild-type tumors in any of the systems analyzed here (Supplementary Figures 1–3). Perhaps GPR56 plays additional roles aside from ECM assembly during cancer progression. Its binding partner, TG2, affects fibronectin-mediated cell adhesion through integrins in an enzyme-independent manner [31,32]. GPR56 might affect cell adhesion through TG2 and its associated factors. In addition, GPR56 was reported recently to inhibit neuronal cell migration by activating RhoA [33]. Cell migration and regulation of Rho GTPases are integral processes during cancer progression [34]. Their regulation by GPR56 might explain the alterations of cancer progression we observed in *Gpr56*−/− mice.

Supplementary Material

Refer to Web version on PubMed Central for supplementary material.

Abbreviations

BFPP	Bilateral frontoparietal polymicrogyria
ECM	Extracellular matrix
GPCR	G protein-coupled receptor
GPR56	G protein-coupled receptor 56
MMTV	Mouse mammary tumor virus
PyMT	Polyoma middle T oncogene
RIPA	Radio-immunoprecipitation assay
TG2	Tissue transglutaminase
TRAMP	Transgenic adenocarcinoma of the mouse prostate

Acknowledgments

We thank Dr. Rulang Jiang and Dr. Sunny Wong for critical readings of the manuscript. We also thank Dr. Sunny Wong for sharing protein lysates from the prostate cancer cell lines. This work was supported by grants from the NIH (U54CA126515, R.O.H), the Virginia and Daniel K Ludwig Fund for Cancer Research (R.O.H), and the Howard Hughes Medical Institute (R.O.H).

Appendices

Supplementary Figures 1, 2, 3 and their legends are included.

References

1. Morgan MR, Humphries MJ, Bass MD. Synergistic control of cell adhesion by integrins and syndecans. Nat Rev Mol Cell Biol. 2007; 8(12):957–969. [PubMed: 17971838]
2. Hynes RO. Integrins: bidirectional, allosteric signaling machines. Cell. 2002; 110(6):673–687. [PubMed: 12297042]
3. Miranti CK, Brugge JS. Sensing the environment: a historical perspective on integrin signal transduction. Nat Cell Biol. 2002; 4(4):E83–E90. [PubMed: 11944041]
4. Streuli CH, Akhtar N. Signal co-operation between integrins and other receptor systems. Biochem J. 2009; 418(3):491–506. [PubMed: 19228122]

5. Lagerstrom MC, Schioth HB. Structural diversity of G protein-coupled receptors and significance for drug discovery. Nat Rev Drug Discov. 2008; 7(4):339–357. [PubMed: 18382464]
6. Stacey M, Chang GW, Davies JQ, et al. The epidermal growth factor-like domains of the human EMR2 receptor mediate cell attachment through chondroitin sulfate glycosaminoglycans. Blood. 2003; 102(8):2916–2924. [PubMed: 12829604]
7. Kwakkenbos MJ, Pouwels W, Matmati M, et al. Expression of the largest CD97 and EMR2 isoforms on leukocytes facilitates a specific interaction with chondroitin sulfate on B cells. J Leukoc Biol. 2005; 77(1):112–119. [PubMed: 15498814]
8. Xu L, Begum S, Hearn JD, et al. GPR56, an atypical G protein-coupled receptor, binds tissue transglutaminase, TG2, and inhibits melanoma tumor growth and metastasis. Proc Natl Acad Sci U S A. 2006; 103(24):9023–9028. [PubMed: 16757564]
9. Wang T, Ward Y, Tian L, et al. CD97, an adhesion receptor on inflammatory cells, stimulates angiogenesis through binding integrin counterreceptors on endothelial cells. Blood. 2005; 105(7): 2836–2844. [PubMed: 15576472]
10. Vallon M, Essler M. Proteolytically processed soluble tumor endothelial marker (TEM) 5 mediates endothelial cell survival during angiogenesis by linking integrin alpha(v)beta3 to glycosaminoglycans. J Biol Chem. 2006; 281(45):34179–34188. [PubMed: 16982628]
11. Lorand L, Graham RM. Transglutaminases: crosslinking enzymes with pleiotropic functions. Nat Rev Mol Cell Biol. 2003; 4(2):140–156. [PubMed: 12563291]
12. Xu L, Hynes RO. GPR56 and TG2: possible roles in suppression of tumor growth by the microenvironment. Cell Cycle. 2007; 6(2):160–165. [PubMed: 17314516]
13. Li S, Jin Z, Koirala S, et al. GPR56 regulates pial basement membrane integrity and cortical lamination. J Neurosci. 2008; 28(22):5817–5826. [PubMed: 18509043]
14. Koirala S, Jin Z, Piao X, et al. GPR56-regulated granule cell adhesion is essential for rostral cerebellar development. J Neurosci. 2009; 29(23):7439–7449. [PubMed: 19515912]
15. Zendman AJ, Cornelissen IM, Weidle UH, et al. TM7XN1, a novel human EGF-TM7-like cDNA, detected with mRNA differential display using human melanoma cell lines with different metastatic potential. FEBS Lett. 1999; 446(2–3):292–298. [PubMed: 10100861]
16. Shashidhar S, Lorente G, Nagavarapu U, et al. GPR56 is a GPCR that is overexpressed in gliomas and functions in tumor cell adhesion. Oncogene. 2005; 24(10):1673–1682. [PubMed: 15674329]
17. Sud N, Sharma R, Ray R, et al. Differential expression of G-protein coupled receptor 56 in human esophageal squamous cell carcinoma. Cancer Lett. 2006; 233(2):265–270. [PubMed: 15916848]
18. Frese KK, Tuveson DA. Maximizing mouse cancer models. Nat Rev Cancer. 2007; 7(9):645–658. [PubMed: 17687385]
19. Greenberg NM, DeMayo F, Finegold MJ, et al. Prostate cancer in a transgenic mouse. Proc Natl Acad Sci U S A. 1995; 92(8):3439–3443. [PubMed: 7724580]
20. Lin EY, Jones JG, Li P, et al. Progression to malignancy in the polyoma middle T oncoprotein mouse breast cancer model provides a reliable model for human diseases. Am J Pathol. 2003; 163(5):2113–2126. [PubMed: 14578209]
21. Chin L, Pomerantz J, Polsky D, et al. Cooperative effects of INK4a and ras in melanoma susceptibility in vivo. Genes Dev. 1997; 11(21):2822–2834. [PubMed: 9353252]
22. Kaplan-Lefko PJ, Chen TM, Ittmann MM, et al. Pathobiology of autochthonous prostate cancer in a pre-clinical transgenic mouse model. Prostate. 2003; 55(3):219–237. [PubMed: 12692788]
23. Wong SY, Haack H, Kissil JL, et al. Protein 4.1B suppresses prostate cancer progression and metastasis. Proc Natl Acad Sci U S A. 2007; 104(31):12784–12789. [PubMed: 17640904]
24. Gingrich JR, Barrios RJ, Morton RA, et al. Metastatic prostate cancer in a transgenic mouse. Cancer Res. 1996; 56(18):4096–4102. [PubMed: 8797572]
25. Hurwitz AA, Foster BA, Allison JP, et al. The TRAMP mouse as a model for prostate cancer. Curr Protoc Immunol. 2001; Chapter 20(Unit 20):5. [PubMed: 18432778]
26. Sharpless E, Chin L. The INK4a/ARF locus and melanoma. Oncogene. 2003; 22(20):3092–3098. [PubMed: 12789286]

27. Galle J, Aust G, Schaller G, et al. Individual cell-based models of the spatial-temporal organization of multicellular systems--achievements and limitations. Cytometry A. 2006; 69(7):704–710. [PubMed: 16807896]

28. Nishimori H, Shiratsuchi T, Urano T, et al. A novel brain-specific p53-target gene, BAI1, containing thrombospondin type 1 repeats inhibits experimental angiogenesis. Oncogene. 1997; 15(18):2145–2150. [PubMed: 9393972]

29. Terskikh AV, Easterday MC, Li L, et al. From hematopoiesis to neuropoiesis: evidence of overlapping genetic programs. Proc Natl Acad Sci U S A. 2001; 98(14):7934–7939. [PubMed: 11438738]

30. Terskikh AV, Miyamoto T, Chang C, et al. Gene expression analysis of purified hematopoietic stem cells and committed progenitors. Blood. 2003; 102(1):94–101. [PubMed: 12623852]

31. Akimov SS, Krylov D, Fleischman LF, et al. Tissue transglutaminase is an integrin-binding adhesion coreceptor for fibronectin. J Cell Biol. 2000; 148(4):825–838. [PubMed: 10684262]

32. Akimov SS, Belkin AM. Cell surface tissue transglutaminase is involved in adhesion and migration of monocytic cells on fibronectin. Blood. 2001; 98(5):1567–1576. [PubMed: 11520809]

33. Iguchi T, Sakata K, Yoshizaki K, et al. Orphan G protein-coupled receptor GPR56 regulates neural progenitor cell migration via a G alpha 12/13 and Rho pathway. J Biol Chem. 2008; 283(21): 14469–14478. [PubMed: 18378689]

34. Hall A. The cytoskeleton and cancer. Cancer Metastasis Rev. 2009; 28(1–2):5–14. [PubMed: 19153674]

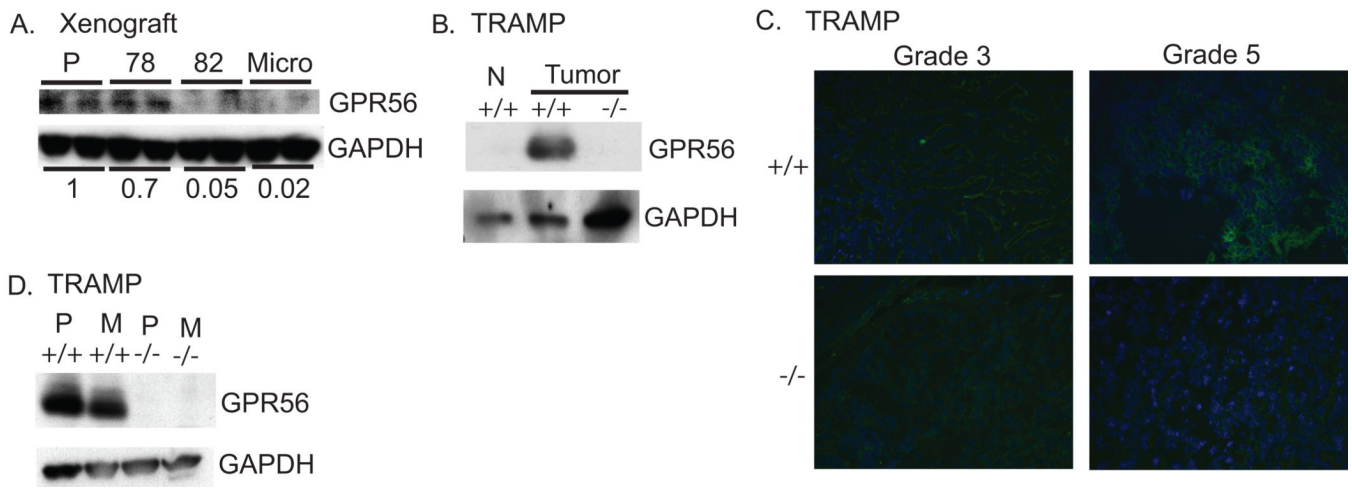

Figure 1. Expression of GPR56 in mouse models of prostate cancer

A. Xenograft model. GPR56 protein was diminished in tumor samples from metastatic prostate cancer cell lines, relative to those from poorly metastatic cells. P (parental) and #78 cells are poorly metastatic, pMicro cells have intermediate metastatic ability, and #82 cells are highly metastatic [23]. These cells were injected into immunodeficient mice subcutaneously, and the tumors were lysed and probed with an antibody that recognizes the C-terminus of GPR56 (anti-GPRC antibody) or mouse anti-GAPDH as a loading control (see Materials and Methods). The relative protein level of GPR56 in each sample is shown at the bottom of the panel.

B. TRAMP model. The expression of GPR56 was induced during prostate cancer progression of TRAMP mice. Protein lysates from normal prostates or prostate tumors from TRAMP mice were probed with anti-GPRC antibody on western blots. GAPDH was used as a loading control. The C-terminus of GPR56 was abundantly expressed in prostate tumors from the TRAMP mice, but was not detectable in normal prostates of their non-transgenic siblings. Prostate tumors from *Gpr56−/−* TRAMP mice were used as a negative control to confirm the specificity of the anti-GPRC antibody. N: normal prostate.

C. Immunohistochemical analyses showed that GPR56 protein levels were increased in the prostate cancer of higher grades from TRAMP mice. Frozen sections from prostate cancer of grade 3 or 5 were probed with anti-GPRC antibody (green) and DAPI (blue) for DNA.

D. In TRAMP mice, high GPR56 expression level is maintained in the lymph node metastases as in the primary tumor it was originated. Protein lysates from a lymph node metastasis and the primary tumor were probed with anti-GPRC antibody or anti-GAPDH antibody on western blots. P: primary tumor; M: lymph node metastasis.

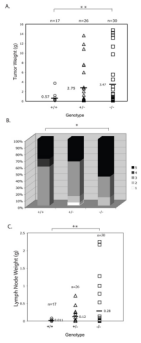

Figure 2. GPR56 inhibited prostate cancer progression in TRAMP mice on a mixed genetic background

Gpr56−/− mice were crossed with TRAMP mice to study the effects of GPR56 on prostate cancer development. The transgenic offspring were sacrificed at the ages of 20 weeks and their prostates and lumbar lymph nodes were dissected and analyzed.

A. Prostate tumor weights in transgenic *Gpr*56−/− mice were significantly increased relative to those in wild-type mice. **: $p < 0.01$, *Mann-Whitney* test. Prostate tumor weights in transgenic Gpr56+/− mice were also increased relative to wild-type mice, but the difference was not statistically significant ($p > 0.05$, *Mann-Whitney* test).

B. A larger proportion of prostate tumors in *Gpr56−/−* mice were at the highest grade (grade 5) than those in wild-type mice. *: $p = 0.05$, *Fisher Exact* test for distribution of grade 3 and grade 5 tumors in wild-type and *Gpr56−/−* mice.

C. The weights of lymph node metastases were significantly increased in *Gpr56−/−* mice relative to wild-type mice. **: $p < 0.01$, *Mann-Whitney* test. The weights of lymph node metastases in *Gpr56+/−* mice were also increased relative to those in wild-type mice, but the difference was not statistically significant ($p > 0.05$, *Mann-Whitney* test).

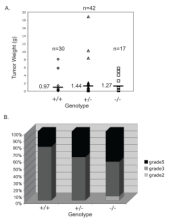

Figure 3. GPR56 did not affect prostate cancer progression in TRAMP; C57BL/6 mice

Gpr56−/− mice were backcrossed into the C57BL/6 background for five generations and then crossed with TRAMP mice (which were on C57BL/6 background). Experimental animals were sacrificed at 25 weeks. Prostate tumor weights (A) and grades (B) were not affected by the absence of *Gpr56* ($p > 0.05$, *Mann-Whitney* test for tumor weights and *Fisher Exact* test for tumor grades).

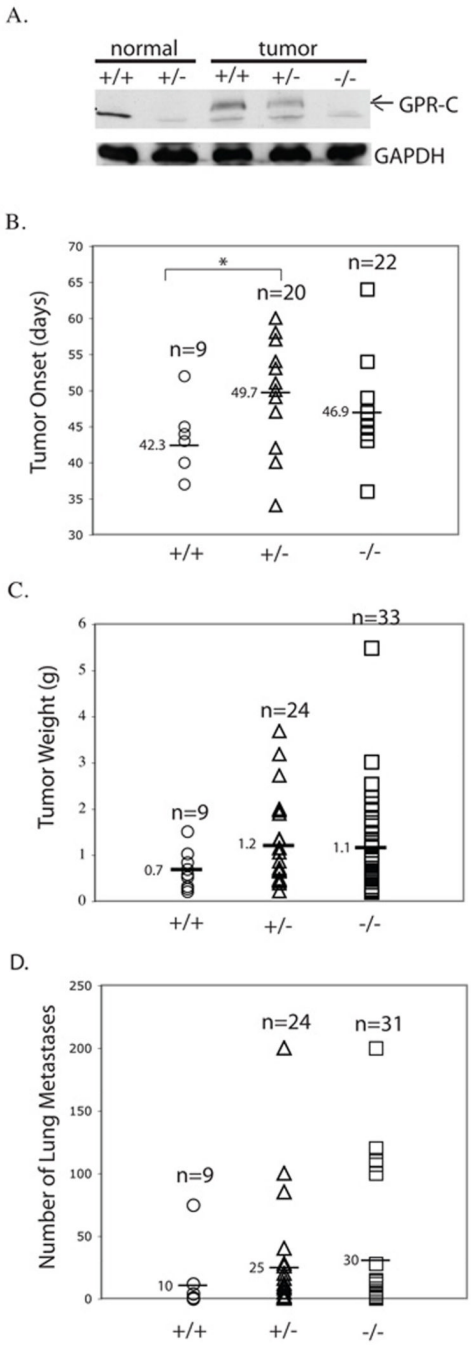

Figure 4. *Gpr56* had marginal effects on mammary tumor onset, but not progression in MMTV-PyMT mice

Gpr56−/− mice were crossed with the mammary tumor model, MMTV-PyMT, and the progenies were analyzed for their mammary tumor progression. A. GPR56 protein levels in the MMTV-PyMT mice were increased in mammary tumors compared with normal mammary glands. B. Tumor onset was significantly delayed in *Gpr56*+/− mice compared with that in wild-type mice. *: $p < 0.05$, Student's *t*-test. C. Tumor masses did not differ among the wild-type, *Gpr56*+/−, and *Gpr56*−/− mice of 14 weeks. $p > 0.05$, *Mann-Whitney* test. D. The numbers of lung metastases did not vary significantly among the *Gpr56*+/+, *Gpr56*+/−, and *Gpr56*−/− MMTV-PyMT mice. $p > 0.05$, *Mann-Whitney* test.

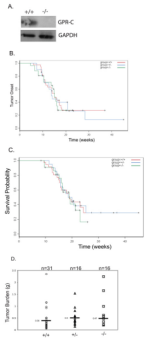

Figure 5. GPR56 deficiency did not affect melanoma progression in *Ink4a/Arf−/−tyr-Hras* mice

Gpr56−/− mice were crossed with the melanoma mouse model, *Ink4a/Arf−/−tyr-Hras* mice, and the progenies were analyzed for melanoma development. GPR56 is expressed in melanomas arisen from these mice (A). There is no significant difference in tumor onset (B), survival probability (C) and tumor burden (D) among the *Gpr56+/+*, *Gpr56+/−*, and *Gpr56−/−* mice. Tumor onset was scored as the time when melanoma was first detected. Tumor burden was scored as the total tumor weight from each animal at the time of its death. $p > 0.05$, Mann-Whitney test for tumor burden, and log-rank tests for tumor onset and survival.